DOI: 10.1002/cbic.200800057

Enhanced Complexity and Catalytic Efficiency in the Hydrolysis of Phosphate Diesters by Rationally Designed Helix-Loop-Helix Motifs

Jesus Razkin,*[c] Johan Lindgren,[a] Helena Nilsson,[b] and Lars Baltzer*[a]

HJ1, a 42-residue peptide that folds into a helix-loop-helix motif and dimerizes to form a four-helix bundle, successfully catalyzes the cleavage of "early stage" DNA model substrates in an aqueous solution at pH 7.0, with a rate enhancement in the hydrolysis of heptyl 4-nitrophenyl phosphate of over three orders of magnitude over that of the imidazole-catalyzed reaction, $k_2(HJ1)/k_2(Im) = 3135$. The second-order rate constant, $k_2(HJ1)$ was determined to be $1.58 \times 10^{-4}\ M^{-1}s^{-1}$. The catalyst successfully assembles residues that in a single elementary reaction step are capable of general-acid and general-base catalysis as well as transition state stabilization and proximity effects. The reactivity achieved with the HJ1 polypeptide, rationally designed to catalyze the hydrolysis of phosphodiesters, is based on two histidine residues flanked by four arginines and two adjacent tyrosine residues, all located on the surface of a helix-loop-helix motif. The introduction of Tyr residues close to the catalytic site improves efficiency, in the cleavage of activated aryl alkyl phosphates as well as less activated dialkyl phosphates. HJ1 is also effective in the cleavage of an RNA-mimic substrate, uridine-3'-2,2,2-trichloroethyl phosphate (leaving group $pK_a = 12.3$) with a second-order rate constant of $8.23 \times 10^{-4}\ M^{-1}s^{-1}$ in aqueous solution at pH 7.0, some 500 times faster than the reaction catalyzed by imidazole, $k_2(HJ1)/k_2(Im) = 496$.

Introduction

The engineering of novel man-made catalysts tailored for specific functions with the efficiency and selectivity of natural enzymes remains a considerable challenge in spite of the large efforts invested in this intriguing and important problem. The main difficulty is encountered at the molecular level, at which the bringing together of several residues to perform several catalytic functions simultaneously in the same elementary, and rate limiting, reaction step requires the design of highly complex structures. In this context, a key role is played by de novo designed proteins.[1–2] They can accommodate both natural and non-natural amino acids, organized in a variety of different geometries, to generate many potential catalytic sites for important chemical reactions, to test concepts of catalysis in a rational way. We reported previously on the reactivity of functionalized helix-loop-helix dimers[3] and have now embarked on a search for new and efficient catalysts for the hydrolysis of polynucleotides, using four-helix bundle polypeptides as simple but powerful scaffolds with the goal to combine general-acid/general-base catalysis with substrate binding and transition state stabilization by rational design.

Transmembrane signaling and cellular energy regulation, as well as many biosynthesis pathways,[4] take advantage of phosphorylation reactions, and phosphodiester bonds constitute the backbones of DNA and RNA. Nucleic acids have become a key target in drug development because of their role in the transmission of genetic information and the expression of proteins in vivo. The successful design of artificial nucleases with specific cleaving activity could thus provide powerful therapeutic tools. The phosphoester linkages involved are extremely stable and resistant to hydrolysis.[5] Enzymes that have evolved to catalyze their hydrolysis are among the most efficient known, with rate enhancements of eighteen orders of magnitude or more, stemming from a combination of general-acid and general-base catalysis, nucleophilic catalysis, transition state stabilization, and proximity effects. Thus the design of nucleases that match the efficiency of natural ones constitutes a formidable but interesting challenge.[6]

Metallonucleases have so far attracted the most interest as model catalysts[7] because metal ions are often found in the active sites of natural enzymes that cleave phosphodiester bonds.[8] The advantages of using metals for biochemical reactions arise from their affinity for basic nitrogen and oxygen donor ligands, their capacity to support large aromatic architectures capable of π interactions with the nucleic acid building blocks, their ability to directly hydrolyze phosphodiester linkages, and the possibility of promoting redox chemistry or

[a] *J. Lindgren, Prof. L. Baltzer*
Department of Biochemistry and Organic Chemistry, Uppsala University
Box 576, 75123 Uppsala (Sweden)
Fax: (+46) 18-471-3818
E-mail: lars.baltzer@biorg.uu.se

[b] *H. Nilsson*
Department of Organic Chemistry, IFM, Linköping University
58183 Linköping (Sweden)

[c] *Dr. J. Razkin*
Department of Applied Chemistry, Public University of Navarra
31006 Pamplona, Navarra (Spain)
Fax: (+34) 948-169606
E-mail: jrazk@unavarra.es

Supporting information for this article is available on the WWW under http://www.chembiochem.org or from the author.

generating reactive oxygen-derived species.[9] Yet, there are also problems still to be solved, as the time-dependent exchange reactions of metal ions,[7a] the slow penetration into cells of metal ion chelates tethered to oligonucleotide based drugs,[7a] or the need for more efficient binding to the target nucleic acid,[7b,c] often too dependent on direct coordination to the metal center.

Remarkable results in terms of cleavage activity as well as sequence recognition have also been achieved with metal-free catalysts: diethylenetriamine-ODN (oligodeoxyribonucleotides),[10] imidazole containing ODNs,[11] peptides conjugated to ODNs,[12] methanephosphonate ODNs with an imidazole/amino or diimidazole cleaving agent,[13] a PNA (peptide nucleic acid) conjugate of neamine,[14] and a PNA-linked diethylenetriamine moiety.[15] Recently, it has been shown that tris(2-aminobenzimidazoles) attached to DNA oligonucleotides act as efficient nucleases, with substrate and site selectivity as well as saturation kinetics, demonstrating the catalytic power of metal-free systems.[16]

In this context, we have shown[17] that HNI, a 42-residue peptide that folds into a helix-loop-helix motif and dimerizes in an antiparallel fashion to form a four-helix bundle, successfully catalyzes the intramolecular phosphoryl transfer reaction and cyclization of an RNA-mimic substrate, uridine-3′-2,2,2-trichloroethyl phosphate[18] (**1**) in aqueous solution at pH 7.0, with a rate enhancement of more than two orders of magnitude over that of the imidazole-catalyzed reaction, k_2(HNI)/k_2(Im) = 252.

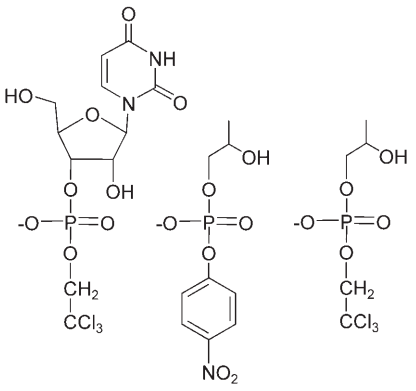

1 **2** **3**

The key to efficient catalysis is to combine several catalytic functions acting in the rate-limiting elementary reaction step. The catalyst HNI was able to combine general-acid/general-base catalysis with transition stabilization. However, substrate binding was not observed. We believe that it is ultimately the systematic introduction of catalytic components in scaffolds of high complexity that will bring designed catalysts to a level of efficiency that matches those of native enzymes.

We report herein on the catalysis of cleavage of a series of activated alkyl aryl phosphate diesters **4**–**7** as "early stage" DNA model substrates executed by de novo designed folded polypeptides. The lack of the 2′-OH group of RNA-mimicking

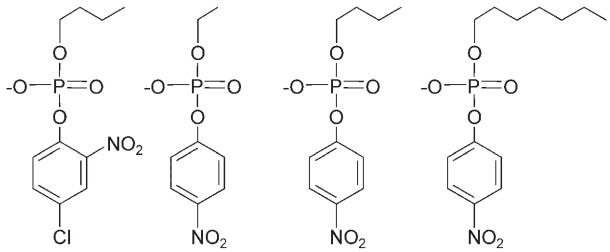

4 **5** **6** **7**

substrates increases the level of complexity needed for DNA hydrolysis, as the nucleophile that attacks the phosphate ester has to be provided by the catalyst. Tyrosine residues were introduced close to the active site designed for RNA hydrolysis and improved catalysis of cleavage of alkyl aryl phosphates has been achieved representing an important advance in rational catalyst design. We also wish to report that we have used the hydrophobic character of the helix-loop-helix dimer and obtained productive binding of hydrophobic substrates and enhanced catalytic efficiency.

Results and Discussion

Our understanding of how to design polypeptide catalysts with enzyme-like activity remains modest because of the challenge of organizing sophisticated reactive sites in well-defined geometries in three-dimensional space. Nevertheless, the results obtained in studies of simple model catalysts suggest that several catalytic functions may be implemented co-operatively in scaffolds with complexities that are modest in comparison with those of native protein catalysts.

We have focused on the development of the four-helix bundle motif, a robust but sophisticated peptide scaffold. It is conveniently synthesized with site-selective introduction of functionality (Figure 1) and it ensures water solubility for covalently linked groups. Folded polypeptides provide a high degree of design versatility and ample possibilities to systematically modify active site geometries for structure–activity studies.

We have demonstrated previously[17] using the HNI peptide that it is possible to implement a combination of general-acid/general-base catalysis and transition state stabilization in the cleavage of the activated "early stage" RNA model 2-hydroxypropyl *p*-nitrophenylphosphate, HPNP (**2**), the less reactive substrate 2-hydroxypropyl-2,2,2-trichloroethylphosphate (**3**), and the more realistic RNA-mimic, uridine-3′-2,2,2-trichloroethyl phosphate (**1**). Those results encouraged us to optimize and refine the catalytic site of the polypeptide further and to test the catalysis of the cleavage of more difficult targets, such as DNA analogues. We have now introduced into the catalyst a nucleophile positioned to attack the phosphate ester, and set out to explore the possibility of obtaining substrate binding, the hallmark of enzyme catalysis.

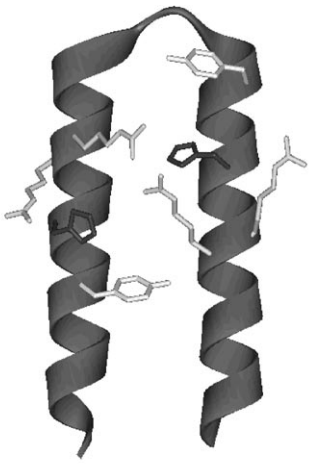

Ac-N-A-A-D-Nle-E-A-Y^{8}-I-K-H^{11}-L-A-R^{14}-R^{15}-Nle-A-A-K-
G-P-V-D-
H_2N-G-A-R-A-F-A-E-F-R^{34}-R^{33}-A-L-H^{30}-E-A-Nle-Y^{26}-A-A-

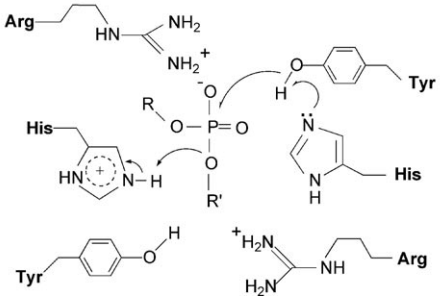

Figure 1. The modeled structure of the helix-loop-helix motif and the amino acid sequence of HJ1. The one letter code for the amino acids is used; Nle is norleucine. The C-terminal is amidated and the N-terminal is acetylated. Only the side chains of the residues designed for catalysis are shown. The dimer is the catalytically active peptide but only the monomer is shown for clarity of presentation. In solution, the dimer dissociates at low-μM concentration to form unordered and catalytically inactive monomers. The insert illustrates one of the possible interactions between active site residues and substrate.

Catalyst design

The designs of the peptides reported herein, HJ0–HJ3 were based on the design of HNI (H. Nilsson, J. Razkin, and L. Baltzer, unpublished), which was based on the sequence of the de novo designed template polypeptide SA-42[19] and on the understanding that evolved from extensive studies of structure and dynamics of the parent peptide and of the polypeptides[20] derived from it. All these 42-residue sequences were designed to fold into two amphiphilic helical segments linked by a four-residue loop, form a hairpin helix-loop-helix motif, and dimerize in an antiparallel mode to form a four-helix bundle.[19]

The design of those peptides is based on the heptad repeat pattern[2a] $(a\text{-}b\text{-}c\text{-}d\text{-}e\text{-}f\text{-}g)_n$ in which the residues in the a and d positions form the hydrophobic core, those in the c and g positions form the exposed surface of the dimmer, and the residues in the b and e positions are at the dimer interface and control dimerization. The main arguments to select the amino acids were their propensities for secondary structure formation[21] and their ability to stabilize the helical folded structure by formation of salt bridges and by stabilization of the helix dipole moment.[2] The C and N termini were capped by amidation and acylation, respectively. Shape complementary hydrophobic interfaces were obtained by judicious choices of leucine, isoleucine, norleucine, and phenylalanine residues to form hydrophobic interactions between amphiphilic helices upon folding, thus driving the formation of the helix-loop-helix hairpin and its dimerization.

The reactive sites of the HJ sequences (Figure 2) were based on that of HNI, which has been shown previously to efficiently catalyze cyclization reactions of RNA mimics.[17] The sequences

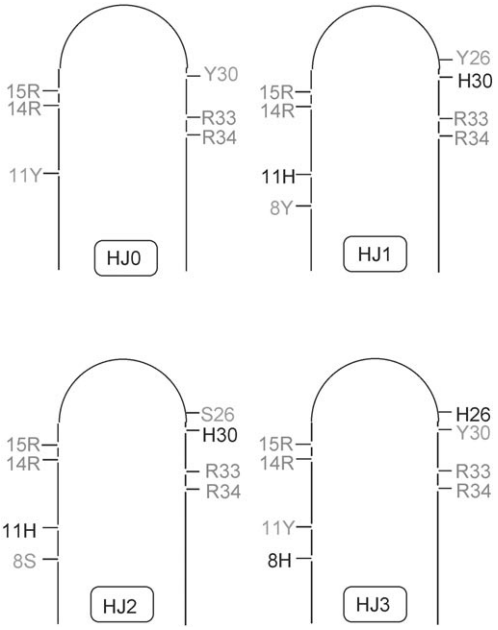

Figure 2. Schematic representation of the HJ0-HJ3 peptides. Only the residues incorporated for catalysis and the amino acids that differ from those of the sequence of HNI are shown.

HJ0–HJ2 deviate from that of HNI in only two positions, and the sequence HJ3 deviates in only four positions. The fact that the cyclization of uridine-3′-2,2,2-trichloroethyl phosphate (**1**) catalyzed by HNI did not follow saturation kinetics[17] in the concentration range from 5–40 mM of substrate pointed clearly to the need for improved substrate binding as one key factor in the development of the catalyst. Another key component required for the hydrolysis of DNA mimics was nucleophilic assistance and Tyr residues are capable of providing nucleophilic catalysis through its hydroxyl group. Thus, two Tyr residues were introduced close to the catalytic site, to allow hydrophobic interactions with the substrates and in positions to provide nucleophilic catalysis in phosphodiester hydrolysis.

HJ0 is a reference sequence in which the His residues in positions 11 and 30 of HNI were replaced by Tyr residues to probe the unique role of the histidines in the active site. In the sequence HJ1, tyrosine residues were incorporated in positions that flank the His groups, that is, in positions 8 and 26, to supplement and improve on the catalytic site of HNI and investi-

gate the possibility of providing nucleophilic attack on the phosphate group and enable the efficient hydrolysis of DNA-mimicking substrates. In HJ2 the tyrosine residues of HJ1 were replaced by serines to investigate the structure–activity relationship of the potential nucleophiles and in HJ3 the positions of tyrosine and histidine residues were reversed in comparison with those in the sequence of HJ1. HJ3 was to act as a negative control and probe the requirements for specific positioning of catalytically active groups in the active site. The choice of tyrosine residues was guided by the considerations described above and also by the frequent occurrence of tyrosine residues in binding sites in proteins.

As a result of their large sequence homology with the parent polypeptides, which were extensively characterized[19–20] by NMR and CD spectroscopy and by analytical ultracentrifugation, a detailed analysis of the solution structures of the HJ series of peptides has not been carried out. We assume, based on the similarities with the parent sequences, that HJ0–HJ3 adopt the same fold. The mean residue ellipticity of a polypeptide at 222 nm, Θ_{222}, is an established probe of helix formation and a good reporter of dimer formation for the sequences mentioned here. All sequences derived from the SA-42 family of peptides show strong concentration dependence and low helical content in the monomeric state. The CD spectrum of HJ1 shows the hallmarks of a helical protein,[22] with minima at 208 and 222 nm (see the Supporting Information). The mean residue ellipticity of HJ1 at 222 nm was $-22\,970^\circ\,cm^2\,dmol^{-1}$ at a concentration of 0.226 mM, pH 7.0, and room temperature, which is well within the range of other sequences derived from SA-42 that have been shown to fold into helix-loop-helix dimers. The CD spectrum of HNI also shows the minima at 208 and 222 nm typical of helical sequences and the mean residue ellipticity at 222 nm at 0.5 mM concentration and pH 7.0 was $-20\,390\,deg\,cm^2\,dmol^{-1}$. We conclude therefore, that HJ1 folds under those conditions into a helix-loop-helix motif that dimerizes to form a four-helix bundle. The peptides were synthesized by solid-phase peptide synthesis on an automated peptide synthesizer, using standard Fmoc protocols (9-fluorenylmethoxycarbonyl protection group). They were purified by reversed-phase HPLC and identified using MALDI-TOF mass spectrometry (Supporting Information).

Substrate design

Uridine-3′-2,2,2-trichloroethyl phosphate (**1**) has been used as a mimic of RNA because of its leaving group pK_a of 12.3,[23] which is close to that of a ribose 5′-OH, 14.3[24] and more than five pK_a units higher than the pK_a of *p*-nitrophenol, which is 7.1.[25] Its hydrolysis is energetically less favorable than that of commonly used activated model substrates with *p*-nitrophenyl leaving groups and represents, therefore, a more realistic model substrate for the evaluation of catalysts capable of cleaving RNA. It is intramolecularly cyclized under the same conditions as HPNP, and under the release of 2,2,2-trichloroethanol. The reaction mimics the first step in enzyme-catalyzed RNA hydrolysis in which the 2′-OH group attacks the phosphorus atom to form the cyclic intermediate under the release of the 5′-OH from the neighboring nucleotide. It has the nucleophile in a fixed position relative to the phosphate group as in RNA and is therefore reactive enough for its cyclization to be conveniently studied by standard kinetic methods. Substrates (**2**) and (**3**) are also mimics of RNA, the former an activated one and the latter less so, due to the higher pK_a of the trichloroethyl leaving group. Both of these substrates have rotatable bonds and therefore less preorganization than **1** in which the 2′-OH is in position for nucleophilic attack. Substrate **3** is fairly unreactive.

Substrates that mimic DNA have no intramolecular nucleophile to attack the phosphate ester and the nucleophile has to be provided by the catalyst. The attack by water or the hydroxide ion is slow at neutral pH. DNA mimics are therefore inherently less reactive, everything else being equal, than RNA mimics. A set of nitrophenyl phosphate diesters (compounds **4**–**7**) was prepared to be used as activated "early stage" DNA models to test the efficiency of the designed peptide catalysts in DNA cleavage. As there is no intramolecular nucleophile, the reduction of the rotational degrees of freedom is unimportant in the substrates. Because of the lower inherent reactivity of DNA mimics in comparison with RNA mimics, the use of more realistic and less reactive substrates has to await the development of more mature catalysts.

The structures of the substrates used here were inspired by that of the simple RNA analogue HPNP (**2**) but without its characteristic 2-hydroxy group, thus mimicking the absence of intramolecular nucleophilic assistance found in DNA hydrolysis. Linear primary alcohols with increasing numbers of carbon atoms were selected to form the phosphate diesters **4**–**7** in an attempt to achieve substrate binding through hydrophobic interactions with the catalyst. The selected substrates thus constitute a set of nucleic acid models showing a systematic variation in the degree of hydrophobicity but with rather modest variation in inherent reactivity. In **4** a more reactive leaving group (pK_a = 6.4)[25] was introduced to allow a comparison with **6** that is equally hydrophobic but less reactive. Two activated phosphate monoesters were also synthesized, *p*-nitrophenylphosphate and 2,4-dinitrophenylphosphate, but their background hydrolysis was too fast to make studies of catalysis meaningful and they were abandoned.

Three activated esters 4-nitrophenyl acetate (**8**), 4-nitrophenyl butyrate (**9**), and 4-nitrophenyl octanoate (**10**) were studied in order to investigate the esterase activity as well as self-catalyzed modification of the catalysts HJ0–HJ3.

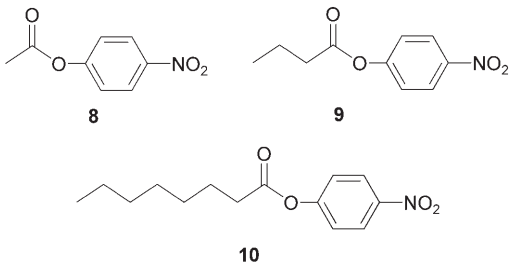

Catalysis of hydrolysis of substrates that mimic DNA

The four-helix bundle is a versatile scaffold where several catalytically active residues can be incorporated in predetermined positions. Having demonstrated previously the capacity of HNI for catalyzing the cyclization of substrates **1**–**3** with considerable efficiency, we decided to turn to an even more ambitious goal, the hydrolysis of phosphate diesters that mimic DNA in which no intramolecular nucleophile is available. In addition, we wished to probe the use of hydrophobic interactions between substrates having an aliphatic substituent and hydrophobic groups in the polypeptide catalyst to enhance the catalytic efficiency by exploiting proximity effects. Tyrosine residues were incorporated close to the active site designed previously for the catalysis of cyclization of RNA models. In this site, arginine residues were introduced to bind with differential affinities to the negatively charged phosphate groups of the substrates and to the even more negatively charged transition states by electrostatic interactions and hydrogen bonding. The reactive site was further composed of two histidine residues to provide nucleophilic, general-acid and/or general-base catalysis, Figure 1. The protonated and unprotonated forms of the imidazole groups are capable of binding substrates, intermediates, and transition states in addition to providing general-acid, general-base catalysis, as they are good proton donors and acceptors with p*K*a values at around seven. We found[17] that the catalyst HNI equipped with this reactive site was capable of catalyzing the cyclization of activated and poorly activated phosphate diesters with more than two orders of magnitude of rate enhancement over that of the imidazole-catalyzed reaction. The reactivity achieved with the designed polypeptide HNI was probably due to a combination of general-acid and general acid-base catalysis, as suggested by the pH dependence and the observed kinetic solvent isotope effect, as well as to transition state stabilization. There was no evidence for substrate binding.

In addressing the problem of catalyzing the hydrolysis of DNA model substrates, the second-order rate constants were determined for reactions of substrates with almost identical hydrophobicity but different reactivity, and of substrates with almost identical reactivity but different hydrophobicity. For both of these two sets of experiments, peptide catalysts H0–HJ3 with Tyr or Ser residues were compared to HNI, which has no internal nucleophile for DNA hydrolysis. The objective was to evaluate the possibility of obtaining rate enhancements due to binding of hydrophobic substrates as well as to nucleophilic catalysis.

The rates of hydrolysis of **4** and **6** were determined in the presence of the peptide catalysts HNI and HJ0–HJ3, and the second-order rate constants determined in 50 mM HEPES buffer at pH 7.0 and 313 K, Table 1. The two substrates were of essentially identical hydrophobicity but with different reactivity because of the different p*K*a values of the leaving groups. The reactions were conveniently monitored by measuring the increase in absorbance at 405 nm or 424 nm due to the formation of the 4-nitrophenolate or 4-chloro-2-nitrophenolate anions as a function of time, and the rate constants were calculated from the slopes of the linear plots obtained under conditions of initial rates (Figure 3). The slopes of the plots of concentration versus time, after subtraction of the background reaction rates, were divided by the substrate and peptide concentrations to give the second-order rate constants, k_2, an approach that is valid for reactions that do not follow saturation kinetics.

Table 1. Second-order rate constants, k_2 [$M^{-1}s^{-1}$], for the peptide-catalyzed cleavage[a] of **4** and **6**.

Catalyst	**4**	**6**
HNI	5.41×10^{-4}	3.81×10^{-5}
HJ0	1.70×10^{-5}	4.52×10^{-6}
HJ1	5.48×10^{-4}	8.57×10^{-5}
HJ2	4.62×10^{-4}	2.97×10^{-5}
HJ3	2.99×10^{-4}	3.18×10^{-5}

[a] Conditions: 2 mM of substrate, 1 mM of peptide, 313 K, pH 7.0 (50 mM HEPES buffer solution).

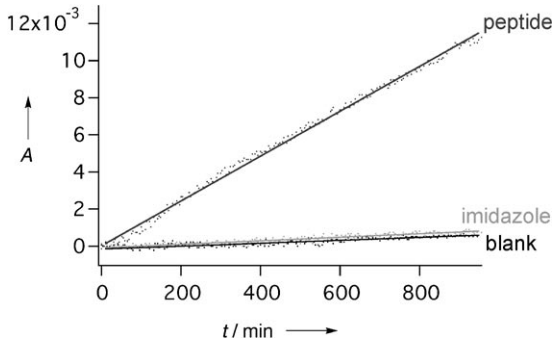

Figure 3. Kinetic profile for the initial rate of cleavage of **7** at pH 7.0 and 313 K by 1 mM HJ1 ("peptide"), by 50 mM imidazole ("imidazole"), and by spontaneous background hydrolysis ("blank"). The best fit of a straight line to the experimental data was obtained by linear regression. The substrate concentration was 1.5 mM in 50 mM HEPES buffer solution and the reactions were followed by vis. spectroscopy at 405 nm.

Substrate **4** is inherently more reactive, by approximately an order of magnitude, than **6**, due to the lower basicity of the leaving group. As expected, the peptide catalyst without His residues, HJ0, was the least efficient in catalyzing the hydrolysis of both substrates, a 30-fold lower second-order rate constant than that of HJ1 in the reaction of **4**, and a 20-fold lower rate constant than HJ1 in the reaction with substrate **6**. However, catalysis and the reactivity of the peptide catalysts is not due to His residues alone, although they contribute general-acid/general-base catalysis. HJ1, the peptide catalyst with Tyr residues incorporated close to the His residues was the most efficient catalyst. It was gratifying to find that the catalysis of HJ1 in comparison to that of HNI was more pronounced for the less reactive substrate **6**, by a factor of 2.2. The importance of catalysis is expected to increase the lower the reactivity of the substrate, whereas very reactive substrates do not need catalysis. Although a factor of 2.2 is not dramatic it suggests

that the Tyr residues contribute to catalysis by nucleophilic assistance or alternatively by hydrogen bonding in the transition state. As the hydrophobicity of the two substrates is almost identical, the difference in reactivity is not likely to be due to hydrophobic interactions.

The two most efficient catalysts HJ1 and HNI were both studied with regards to their capacity for catalyzing the hydrolysis of substrates **5**, **6**, and **7**, in which the hydrophobicity was systematically varied. The second-order rate constants shown in Table 2 reveal that, in general, the more hydrophobic the substrate the faster the reaction, in spite of the fact that the intrinsic reactivity is not expected to be very different. The only factor affecting the relative intrinsic reactivities of **5**, **6**, and **7**, is the difference in inductive effects by the aliphatic substituents on the p*K*a of the alcohols, and that difference is expected to be insignificant. Again, the reaction is faster when catalyzed by HJ1 than by HNI in all cases and more so for the least reactive substrate. The hydrophobic effects are not due to interactions with the aromatic rings of Tyr residues, as the rate constants increase more with increased hydrophobicity also in the reactions catalyzed by HNI where no tyrosines are present. Instead, it is most likely that the longer aliphatic chains interact better with the hydrophobic core of the folded polypeptides, an effect observed previously in the hydrolysis of activated ester substrates.[3]

Table 2. Second-order rate constants, k_2 [$M^{-1}s^{-1}$], for the HNI- and HJ1-catalyzed cleavage[a] of **5**–**7**.

Catalyst	**5**	**6**	**7**
HNI	0.74×10^{-5}	3.81×10^{-5}	1.01×10^{-4}
HJ1	4.04×10^{-5}	8.57×10^{-5}	1.58×10^{-4}

[a] Conditions: 1–2.2 mM of substrate, 1 mM of peptide, 313 K, pH 7.0 (50 mM HEPES buffer solution).

Table 3. Second-order rate constants, k_2 [$M^{-1}s^{-1}$], and rate enhancements for the imidazole, HNI- and HJ1-catalyzed cleavage[a] of **7**.

Catalyst	**5**	**7**	Rate enhancement k_2(Pep)/k_2(Im)
imidazole	9.48×10^{-8}	5.04×10^{-8}	
HNI	0.74×10^{-5}	1.01×10^{-4}	78/2004
HJ1	4.04×10^{-5}	1.58×10^{-4}	426/3135
Rate enhancement k_2(HJ1)/k_2(HNI)	5.46	1.56	

[a] Conditions: 1–2.2 mM of substrate, 1 mM of peptide, 50 mM of imidazole, 313 K, pH 7.0 (50 mM HEPES buffer solution).

The largest difference between HJ1 and HNI was observed for catalysis of hydrolysis of the substrate with the shortest aliphatic substituent, **5**, with a rate constant ratio of 5.5. The ratio is significant and suggests strongly that one or both of the Tyr residues contribute to catalysis by nucleophilic assistance, although a hydrogen bond to the leaving group can not be ruled out.

The catalytic efficiency of HJ1

In order to evaluate the efficiency of catalysis, a reference reaction was chosen for comparison. The active sites of HJ1 and HNI contain Arg, His, and in the case of HJ1, Tyr residues. The functional group of Arg is the guanidino residue, a commonly used denaturant. It has a high p*K*a value in aqueous solution. It is ionized at neutral pH and therefore exerts a salt effect on the reaction in addition to denaturing the catalyst. In principle, guanidinium chloride could be used as a reference but the interactions between phosphate and the guanidinium ion are weak and the expected denaturation of the polypeptide scaffold rules out the use of guanidinium chloride as reference. The imidazole residue of the His group was instead chosen for comparison as it is capable of general-acid and general-base catalysis. Thus, we determined the efficiency of both peptides HJ1 and HNI in catalysis of hydrolysis of the least hydrophobic substrate, ethyl 4-nitrophenyl phosphate (**5**) and the most hydrophobic substrate, heptyl 4-nitrophenyl phosphate (**7**), and compared the second-order rate constants to that of imidazole, Table 3. We found that the rate constant ratio, k_2(HJ1)/k_2(Im), for the most hydrophobic substrate was 3135 whereas in the case of HNI the corresponding ratio was 2004. For **5** the rate constant ratio k_2(HJ1)/k_2(Im) was 426, whereas the rate constant ratio k_2(HNI)/k_2(Im) was 78. The relative efficiencies in the catalysis of **7** was k_2(HJ1)/k_2(HNI) = 1.6, whereas in the catalysis of **5** it was 5.5. The catalysis obtained with HJ1, providing a rate enhancement of more than three orders of magnitude in the catalysis of the hydrolysis of **7** compared to imidazole, which constitutes a very interesting result in terms of catalyst design using folded polypeptides, as it demonstrates that it is possible to take advantage of hydrophobic interactions between catalyst and substrate in a productive manner. The result is independent of the reaction to be catalyzed and of general applicability. The relatively small difference in reactivity between HNI and HJ1 implies that in this case catalysis is not influenced by Tyr residues, but by proximity effects due to interactions between hydrophobic substituents and the polypeptide scaffolds. The reactivity difference between HJ1 and HNI in the catalysis of **5** is clearly dependent on the presence of Tyr residues, but not their hydrophobic character as **5** is the least hydrophobic substrate. Instead the results suggest nucleophilic catalysis, or possibly hydrogen bonding in the transition state between the phenolic hydroxyl group of one or two Tyr residues and one or more oxygens in the phosphate group. These two results indicate that the binding of **7** due to hydrophobic interactions and the catalytic function of the Tyr side chains at this stage of catalyst design are mutually exclusive, and not co-operative. In a situation in which co-operativity can be obtained, sizeable rate enhancements are to be expected. A polypeptide sequence in which the Tyr residues of HJ1 were replaced by Phe was synthesized in order to measure directly the effect of the hydroxyl groups. The sequence was

unfortunately only poorly soluble and no kinetic experiments could be carried out.

Salt effects on catalysis

Due to the ionic character of the hydrolysis reaction, in which a negatively charged substrate is converted to an even more negatively charged transition state, which in the peptide-catalyzed reaction interacts with positively charged Arg residues, ionic effects on catalysis are to be expected. As a model reaction, the HNI-catalyzed cyclization of HPNP was used, and the effect of NaCl determined. The second-order rate constants were determined by measuring the pseudo first-order rate constants at three different concentrations of catalyst and plotting them as a function of catalyst concentration. The best fit of a straight line to the experimental results provided the second-order rate constants.

As expected, based on mechanistic arguments, the second-order rate constant for HNI-catalyzed cyclization of HPNP, $k_2 = 3.1\times10^{-5}\,\text{M}^{-1}\text{s}^{-1}$ at 313 K in 50 mM Bis-Tris buffer, pH 7.0, and a substrate concentration of 10 mM, increased somewhat to $k_2 = 5.0\times10^{-5}\,\text{M}^{-1}\text{s}^{-1}$, upon addition of 75 mM NaCl. In the absence of salt the substrate itself gives rise to a salt effect and the second-order rate constant decreases by a factor of more than two in the presence of 10 mM HPNP in comparison with the reaction carried out at a substrate concentration of 2 mM. At a concentration of 20 mM HPNP, k_2 is somewhat lower than that at 2 mM, but higher than at 10 mM. The reaction catalyzed by HNI is clearly affected by the medium, although the interpretation is complex. In contrast, the imidazole-catalyzed reaction is virtually unaffected by the concentration of substrate and NaCl, because the interaction between catalyst and substrate has very little ionic character.

Catalysis of hydrolysis of uridine-3′-2,2,2-trichloroethyl phosphate by HJ1

In view of the similarity in mechanism between reactions that mimic the hydrolysis of RNA and DNA, the catalysts should be interchangeable. In fact, when HJ1 was used to catalyze the cyclization of uridine-3′-2,2,2-trichloroethyl phosphate (**1**) in aqueous solution at pH 7.0 and 313 K, the second-order rate constant was found to be $8.2\times10^{-4}\,\text{M}^{-1}\text{s}^{-1}$, whereas it was $4.2\times10^{-4}\,\text{M}^{-1}\text{s}^{-1}$ under the same conditions for HNI and $1.7\times10^{-6}\,\text{M}^{-1}\text{s}^{-1}$ for the imidazole-catalyzed reaction (Table 4). The rate constant ratio, k_2(HJI)/k_2(HNI), was a factor of two. A rate constant ratio close to 500 (k_2(HJI)/k_2(Im) = 496) relative to imidazole in the catalysis of cyclization of **1** is promising and suggests that further modifications can be used to optimize the catalyst further in a stepwise and rational fashion.

Covalent modification of the peptide catalysts

In view of the fact that the active site of each peptide catalyst had the capacity for transition state stabilization of phosphoryl transfer reactions, we investigated the possibility that the Tyr side chains might in fact become phosphorylated. A mechanism for which nucleophilic catalysis was invoked might be expected to leave some fraction of the catalyst covalently modified, although if the dephosphorylation of the tyrosine side chains was much faster than phosphorylation, no intermediate would build up to detectable concentrations. After completion of the kinetic experiments the peptides were analyzed by MALDI-TOF mass spectrometry. Phosphorylation was not observed for any of the peptide catalysts after reaction with **1**–**7**. It seems that this observation is not compatible with a mechanism in which covalent intermediates are postulated. However, it must be taken into consideration that catalytic machinery that is capable of forming a covalent conjugate in an intermolecular reaction will also be able to hydrolyze it in an intramolecular, and faster, reaction. Thus, very little phosphorylated intermediate would be expected to build up. Although it is possible that the Tyr side chains contribute to transition state stabilization through hydrogen bonding, nucleophilic catalysis seems more likely due to the high nucleophilicity of Tyr residues.

Table 4. Second-order rate constants, k_2 [$\text{M}^{-1}\text{s}^{-1}$], and rate enhancements for the imidazole, HNI- and HJ1-catalyzed cleavage[a] of **1**.

Catalyst	**1**	Rate enhancement k_2(Pep)/k_2(Im)
imidazole	1.66×10^{-6}	
HNI	4.18×10^{-4}	252
HJ1	8.23×10^{-4}	496
Rate enhancement k_2(HJ1)/k_2(HNI)	2	

[a] Conditions: 2 mM of substrate, 1 mM of peptide, 50 mM of imidazole, 313 K, pH 7.0 (50 mM HEPES buffer solution).

In contrast, when the peptides were reacted with activated aliphatic esters **8**–**10** acylation of all peptides was found. Under conditions of equimolecular amounts of peptide and substrate, the level of modification was only partial, but under conditions of excess substrate over peptide, all peptides were monoacylated and di- and tri-acetylated peptides were detected in considerable amounts. The acylation of peptides by activated esters observed herein is in agreement with previous studies[26] showing that these folded four-helix bundle polypeptides are suitable scaffolds for the efficient, site-selective, and stepwise incorporation of acyl groups.

The activated esters **8**–**10** were mainly used to study the capability of the peptides to trap intermediates along the reaction pathway and not to investigate the catalytic activity of the folded polypeptides with regards to ester substrates, because the peptides were not optimized for esterase activity. However, apparent rate constants were determined (Table 5) and again, HJ0, the peptide without His residues, was the slowest whereas the peptides with tyrosines in their sequences, HJ1 and HJ3, were the most efficient in all experiments, both of them better than the parent peptide, HNI. Surprisingly, the peptide in which the positions of His and Tyr (positions 8–11 and 26–30) were interchanged, HJ3, was the most efficient—more than three times faster than HJ1 and almost five times as fast as HNI. The reason that HJ3 was the fastest is probably that there

Table 5. Second-order rate constants, k_2 [$M^{-1}s^{-1}$], for the peptide-catalyzed cleavage[a] of **8**–**10**.

Catalyst	8	9	10
HNI	0.26	0.27	0.27
HJ0	0.15	0.15	0.22
HJ1	0.37	0.30	0.37
HJ2	0.23	0.24	0.28
HJ3	1.26	1.23	1.24

[a] Conditions: 0.25 mM of substrate, 0.25 mM of peptide, 303 K, pH 7.0 (50 mM HEPES buffer solution).

is a direct reaction between the phenolic hydroxyl groups and the active esters, in a site that is catalytically favorable due to the presence of arginines. The aliphatic substituents did not affect reactivity.

The catalytic mechanism

The observation of salt effects and the fact that HJ0, that has no His residues, catalyzes the hydrolysis reaction of phosphodiesters, clearly show that the Arg residues stabilize the transition state of the reaction by electrostatic interactions. The role of the His residues is important and the pH profile has previously been determined to show that the catalyst depends on one residue in its unprotonated form, whereas the kinetic solvent isotope effect demonstrated the occurrence of a strong hydrogen bond in the transition state, that is, general-acid catalysis. These mechanistic investigations were carried out at around neutral pH at which His residues are present both in their protonated and unprotonated forms.

The introduction of Tyr residues gave rise to rate enhancements over those observed with HNI, that carries no tyrosines, by a factor of five in the best case. Whereas this is not a dramatic rate enhancement, it was achieved by rational design and in addition to previous catalytic capacity. The rational introduction of groups capable of such rate enhancements in a stepwise fashion will ultimately lead to powerful catalysts.

With the most hydrophobic substrates, the rate enhancements were the highest, whereas the difference between catalysts with Tyr residues and without, were very small. Here the rate enhancements were most likely due to hydrophobic interactions, although not involving the tyrosines, as HNI and HJ1 were equally effective. The absence of detectable phosphorylation seems to rule out covalent catalysis, in favor of hydrogen bonding in the transition state as the catalytic function of the Tyr residues. However, this need not be true, as discussed above, and this question remains unresolved. The substrates in which the hydrophobicity is the lowest are those in which the difference between HNI and HJ1 is the largest, suggesting that when binding of the substrate is the weakest, the effect of the Tyr is the largest and that the active site is not optimized to take advantage of both factors co-operatively. Ser groups are not as good nucleophiles as Tyr residues, obviously because of the difference in p*K*a but perhaps also because the phenolic hydroxyl group of Tyr is more exposed than that of Ser.

Conclusions

In summary, the results show that it is possible to assemble several catalytically active groups in a folded polypeptide motif in a configuration in which the catalytic functions are additive and thus catalytically active in the same elementary reaction step. Previously, we have reported on the cyclization reaction of RNA-mimicking substrates, catalyzed by an active site based on two Arg and two His residues. Here, we have added two Tyr residues to the catalyst, and taken advantage of the hydrophobic character of the helix-loop-helix motif to study hydrolysis reactions of substrates with increasingly hydrophobic substituents. The rate enhancements obtained due to the introduction of Tyr residues, a factor of 5.5 with an activated aryl alkyl phosphate and a factor of almost 2 with unactivated dialkyl phosphate, relative to those of HNI, which has no Tyr residues, is best explained as a contribution from nucleophilic assistance in the hydrolysis reaction, or alternatively increased hydrogen bonding in the transition state. The design goal of obtaining hydrophobic interactions between Tyr side chains and hydrophobic substrates was not realized. The largest effect on reactivity was observed as a result of increasing the hydrophobicity of phosphate diesters by increasing the number of methylene groups in the aliphatic substituent from two to seven. An increase in the second-order rate constant in the HNI-catalyzed hydrolysis reaction of a factor of 13.5 was obtained, and a factor of 3.8 was obtained in the HJ1-catalyzed reaction. Unfortunately, the active site could not take advantage of the rate enhancements due to Tyr assistance and hydrophobicity co-operatively, but only of one or the other. However, further optimization of these active sites is possible with the further development of de-novo-designed catalysts. Whether it will be possible to arrive at enzyme-like activity by following this strategy remains an open question.

Experimental Section

Instruments and general methods: All aqueous solutions were prepared from distilled and filtered water. ^{1}H, ^{13}C, and ^{31}P NMR spectra were recorded using D_2O or $CDCl_3$ as the solvent on a Varian Mercury 300 or Varian Inova Unity 600 MHz. MALDI-TOF mass spectra were recorded using an Applied Biosystems Voyager DE-STR mass spectrometer. The sample to matrix ratio was 1:10 and α-cyano-4-hydroxycinnamic acid was used as matrix. CD spectra were recorded on an ISA Jobin Yvon-Spex CD6 spectrometer, routinely calibrated with (+)-camphor-10-sulfonic acid, with the samples prepared in buffer solution containing NaCl (0.15 M).

Preparation of substrates: See the Supporting Information.

Kinetics: Rate constants were obtained from experiments performed in parallel using samples prepared from the same substrate, imidazole, or peptide stock solutions to avoid interexperimental errors. They were run at pH 7.0 in 50 mM HEPES buffer. NaCl was added to ensure that the same salt concentration and a constant ionic strength were used in all experiments. The reaction temperature was controlled by a thermostatic bath where tightly stoppered reaction vessels were kept. Peptide samples were prepared as a stock solution by dissolving the lyophilized peptide (25% of water content) in the reaction solvent, adjusting the pH,

and centrifuging prior to being diluted by pipetting to the desired concentrations and transferred to the reaction vessel. In the same way, imidazole and substrates were weighed and dissolved in the reaction solvent, the pH was adjusted, and the required volume taken from the stock solutions. The kinetic measurements started after fast mixing of the reactants, shaking of the vessels, and reintroduction in the thermostated bath, and the evolution of the reaction was followed by the periodical quantification of product formation by way of UV–visible spectroscopy or HPLC analysis. For rate constant calculation, the experimental data points of product concentration were plotted against time, the points were adjusted to lines by linear regression, and the rates calculated from the values of the slopes using Igor Pro software (Wavemetrics Inc.). To obtain the second-order rate constants, k_2, the background reaction was subtracted from the measured pseudo-first-order rates and divided by the initial concentration of catalyst and substrate. Each rate constant is the average of two or three measurements, and the error limits are estimated to be in the range of $\pm 12\%$.

UV/Vis spectroscopy kinetics experiments: All the experiments were carried out at pH 7.0 (50 mM HEPES buffer) and 313, 303, or 298 K, using 0.25–2 mM peptide concentration with 0.25–5 mM substrate concentration in final solutions. A blank experiment was performed at the same time together with a parallel reaction with 50 mM imidazole for comparison in selected cases. NaCl was used to keep a similar ionic strength in all kinetics. The evolution of the reaction was followed by UV spectroscopy monitoring the increase in absorbance due to the formation of the 2,4-dinitrophenolate, 4-nitrophenolate, or 4-chloro-2-nitrophenolate ions. Extinction coefficients: 7785 $M^{-1}cm^{-1}$ for 4-nitrophenyl derivatives (at 405 nm) and 2384 $M^{-1}cm^{-1}$ for 4-chloro-2-nitrophenyl derivatives (at 424 nm).

HPLC kinetic experiments: Reactions were run in H_2O at 313 K (temperature controlled by a thermostatic bath) and pH 7.0 (50 mM HEPES buffer) in tightly stoppered glass bottles with a final volume of 0.6 mL that were periodically shaken. Different samples were prepared with 1 mM peptide (HNI or HJ1), imidazole (50 mM), and the blank experiment (background reaction) with the same concentration of substrate (2 mM), salt (50 mM NaCl), and internal standard (3-nitrobenzenesulfonic acid, sodium salt, 1 mM). The reaction rates were determined by RP-HPLC, measuring the concentration increase of the cyclization product, uridine 2′,3′-cyclic phosphate with detector at 260 nm. Aliquots were withdrawn at suitable intervals and analyzed immediately or kept frozen (liquid nitrogen). Column: Highchrom KR-100-C8–5 (250×4.6 mm, 5 μm particle size). Isocratic elution with 13% acetonitrile in sodium acetate buffer (25 mM, pH 4.3, containing 0.1 M NH_4Cl) as eluent in a 1.5 mL min^{-1} flux. Retention times of product, internal standard, and substrate were 1.89, 5.66, and 8.62 min respectively.

Peptide synthesis: The peptides were synthesized on an automated peptide synthesizer (Pioneer, Applied Biosystems) at a 0.1 mmol scale with standard Fmoc (9-fluorenylmethoxycarbonyl protection group) protocol. The Fmoc protecting group was removed by 20% piperidine in DMF *v/v*. A 0.19 mmol g^{-1} substitution level polymer (PAL-PEG-PS) was used, with an excess of four equivalents of amino acid in each coupling, base-stable protecting groups for side-chain protection and TBTU (0.5 M in DMF) and DIPEA (1 M in DMF) as amino acid activators. Standard coupling times were 60 min, except for Nle and Leu (30 min) and for Gln, Arg, and Asn (90 min). The amino terminal was capped with acetic acid anhydride and carboxy terminal amidated upon cleavage from the resin. When synthesis was completed, the resin was washed with dichloromethane and dried under vacuum. The peptide was then cleaved from the resin and deprotected at RT by treatment with a mixture of TFA/H_2O/ethanedithiol/triisopropyl silane (94:2.5:2.5:1, *v/v/v/v*) for 3 h. It was then filtrated, concentrated (N_2 bubbling), precipitated by addition of cold diethyl ether, washed with diethyl ether, centrifuged, and lyophilized twice. The purification of crude peptides was accomplished by reversed phase HPLC on a semipreparative column (C-8 Kromasil) using isocratic elution with 37% propan-2-ol in water with 0.1% TFA at 10 mL min^{-1} flow rate. The peptides were identified by MALDI-TOF mass spectrometry (Applied Biosystems) and no impurities could be detected by HPLC (detector at 229 nm).

Acknowledgements

The authors wish to thank all ENDEVAN (European Network on the Development of Artificial Nucleases) members, especially A. J. Kirby for his many contributions and his help with the manuscript, and R. Strömberg for suggestions and initial sample of uridine derivative. J.R. was supported by European Commission under the Human Potential Programme (ENDEVAN, HPRN-CT-1999-00008) and financial support was also obtained from the EC, which is gratefully acknowledged.

Keywords: catalysis · de novo design · hydrolysis · peptides · phosphodiesters

[1] a) M. Mutter, S. Vuilleumier, *Angew. Chem.* **1989**, *101*, 551–571; *Angew. Chem. Int. Ed. Engl.* **1989**, *28*, 535–554; b) M. D. Struthers, R. P. Cheng, B. Imperiali, *Science* **1996**, *271*, 342–345; c) B. I. Dahiyat, S. L. Mayo, *Science* **1997**, *278*, 82–87; d) W. D. Kohn, R. S. Hodges, *Trends Biotechnol.* **1998**, *16*, 379–389; e) C. Micklatcher, J. Chmielewski, *Curr. Opin. Chem. Biol.* **1999**, *3*, 724–729; f) E. Lacroix, T. Kortemme, M. Lopez de La Paz, L. Serrano, *Curr. Opin. Struct. Biol.* **1999**, *9*, 487–493; g) B. R. Hill, D. P. Raleigh, A. Lombardi, W. F. DeGrado, *Acc. Chem. Res.* **2000**, *33*, 745–754; h) L. Baltzer, H. Nilsson, J. Nilsson, *Chem. Rev.* **2001**, *101*, 3153–3163; i) J. R. Calhoun, H. Kono, S. Lahr, W. Wang, W. F. DeGrado, J. G. Saven, *J. Mol. Biol.* **2003**, *334*, 1101–1115; j) J. Kaplan, W. F. DeGrado, *Proc. Natl. Acad. Sci. USA* **2004**, *101*, 11566–11570; k) J. R. Calhoun, F. Nastri, O. Maglio, V. Pavone, A. Lombardi, W. F. DeGrado, *Biopolymers* **2005**, *80*, 264–278.

[2] a) J. W. Bryson, S. F. Betz, H. S. Lu, D. J. Suich, H. X. Zhou, K. T. O'Neill, W. F. DeGrado, *Science* **1995**, *270*, 935–941; b) S. F. Betz, W. F. DeGrado, *Biochemistry* **1996**, *35*, 6955–6962.

[3] a) K. Broo, L. Brive, A.-C. Lundh, P. Ahlberg, L. Baltzer, *J. Am. Chem. Soc.* **1996**, *118*, 8172–8173; b) L. Baltzer, A.-C. Lundh, K. Broo, S. Olofsson, P. Ahlberg, *J. Chem. Soc. Perkin Trans. 2* **1996**, 1671–1676; c) K. Broo, M. Allert, L. Andersson, P. Erlandsson, G. Stenhagen, J. Wigström, P. Ahlberg, L. Baltzer, *J. Chem. Soc. Perkin Trans. 2* **1997**, 397–398.

[4] A. Fersht, *Enzyme Structure and Mechanism*, Freeman, New York, **1985**, pp. 259 and 491.

[5] a) J. Kumamoto, J. R. Cox Jr. , F. H. Westheimer, *J. Am. Chem. Soc.* **1956**, *78*, 4858–4860; b) C. A. Bunton, M. M. Mhala, K. G. Oldham, C. A. Vernon, *J. Chem. Soc.* **1960**, 3293–3301; c) A. J. Kirby, M. J. Younas, *Chem. Soc. Rev.* **1970**, *1*, 510–513; d) A. Radzicka, R. Wolfenden, *Science* **1995**, *267*, 90–93; e) R. Wolfenden, C. Ridgway, G. Young, *J. Am. Chem. Soc.* **1998**, *120*, 833–834; f) N. Takeda, M. Shibata, N. Tajima, K. Hirao, M. Komiyama, *J. Org. Chem.* **2000**, *65*, 4391–4396; g) N. H. Williams, P. Wyman, *Chem. Commun.* **2001**, 1268–1269; h) G. K. Schroeder, C. Lad, P. Wyman, N. H. Williams, R. Wolfenden, *Proc. Natl. Acad. Sci. USA* **2006**, *103*, 4052–4055; i) R. Wolfenden, *Chem. Rev.* **2006**, *106*, 3379–3396.

[6] A. J. Kirby, *Angew. Chem.* **1996**, *108*, 770–790; *Angew. Chem. Int. Ed. Engl.* **1996**, *35*, 706–724.

[7] Reviews: a) T. Niittymäki, H. Lönnberg, *Org. Biomol. Chem.* **2006**, *4*, 15–25; b) J. R. Morrow, O. Iranzo, *Curr. Opin. Chem. Biol.* **2004**, *8*, 192–200; c) J. A. Cowan, *Curr. Opin. Chem. Biol.* **2001**, *5*, 634–642; d) R. Häner, *Chimia* **2001**, *55*, 1035–1037; e) M. Komiyama, J. Sumaoka, A. Kuzuya, Y. Yamamoto, *Methods Enzymol.* **2001**, *341*, 455–468; f) S. Mikkola, U. Kau-

kinen, H. Lönnberg, *Cell Biochem. Biophys.* **2001**, *34*, 95–119; g) M. Zenkova, N. Beloglazova, V. Silnikov, V. Vlassov, R. Giege, *Methods Enzymol.* **2001**, *341*, 468–490; h) E. Kimura, *Curr. Opin. Chem. Biol.* **2000**, *4*, 207–213; i) B. Trawick, A. T. Daniher, J. K. Bashkin, *Chem. Rev.* **1998**, *98*, 939–960; j) M. Komiyama, J. Sumaoka, *Curr. Opin. Chem. Biol.* **1998**, *2*, 751–757; k) R. Häner, J. Hall, *Antisense Nucleic Acid Drug Dev.* **1997**, *7*, 423–430; l) M. Komiyama, *J. Biochem.* **1995**, *118*, 665–670.

[8] a) J. Weston, *Chem. Rev.* **2005**, *105*, 2151–2174; b) M. J. Jedrzejas, P. Setlow, *Chem. Rev.* **2001**, *101*, 607–618; c) J. A. Cowan, *Chem. Rev.* **1998**, *98*, 1067–1087; d) D. E. Wilcox, *Chem. Rev.* **1996**, *96*, 2435–2458; e) N. Sträter, W. N. Lipscomb, T. Klabunde, B. Krebs, *Angew. Chem.* **1996**, *108*, 2158–2191; *Angew. Chem. Int. Ed. Engl.Angew. Chem. Int. Ed.* **1996**, *35*, 2024–2055.

[9] L. J. K. Boerner, J. M. Zalesky, *Curr. Opin. Chem. Biol.* **2005**, *9*, 135–144.

[10] a) M. Komiyama, T. Inokava, K. Yoshinari, *Chem. Commun.* **1995**, 77–78; b) M. Komiyama, T. Inokava, *J. Biochem.* **1994**, *116*, 719–720; c) M. Endo, Y. Azuma, Y. Saga, A. Kuzuya, G. Kawai, M. Komiyama, *J. Org. Chem.* **1997**, *62*, 846–852.

[11] a) V. Vlassov, T. Abramova, R. Giege, V. Silnikov, *Antisense Nucleic Acid Drug Dev.* **1997**, *7*, 39–42; b) L. Yurchenko, V. Silnikov, T. Godovikova, G. Shishkin, J.-J. Toulme, V. Vlassov, *Nucleosides Nucleotides* **1997**, *16*, 1721–1725; c) N. G. Beloglazova, V. N. Silnikov, M. A. Zenkova, V. V. Vlassov, *FEBS Lett.* **2000**, *481*, 277–280; d) N. G. Beloglazova, A. Y. Epanchintsev, V. N. Silnikov, M. A. Zenkova, V. V. Vlassov, *Mol. Biol.* **2002**, *36*, 581–588; e) N. G. Beloglazova, M. M. Fabani, M. A. Zenkova, E. V. Bichenkova, N. N. Polushin, V. V. Silnikov, K. T. Douglas, V. V. Vlassov, *Nucleic Acids Res.* **2004**, *32*, 3887–3897.

[12] a) N. L. Mironova, D. V. Pyshnyi, E. M. Ivanova, M. A. Zenkova, H. J. Gross, V. V. Vlassov, *Nucleic Acids Res.* **2004**, *32*, 1928–1936; b) N. L. Mironova, D. V. Pyshnyi, E. M. Ivanova, V. F. Zarytova, M. A. Zenkova, H. J. Gross, V. V. Vlassov, *Russ. Chem. Bull.* **2002**, *51*, 1177–1186; c) N. L. Mironova, Y. I. Boutorine, D. V. Pyshnyi, E. M. Ivanova, M. A. Zenkova, V. V. Vlassov, *Nucleosides Nucleotides Nucleic Acids* **2004**, *23*, 885–890.

[13] a) M. A. Reynolds, T. A. Beck, P. B. Say, D. A. Schwartz, B. P. Dwyer, W. J. Daily, M. M. Vaghefi, M. D. Metzler, R. E. Klem, L. J., Jr. Arnold, *Nucleic Acids Res.* **1996**, *24*, 760–765; b) K. Ushijima, H. Gouzu, K. Hosono, M. Shirakawa, K. Kagosima, K. Takai, H. Takaku, *Biochim. Biophys. Acta, Gen. Subj.* **1998**, *1379*, 217–223.

[14] E. Riguet, S. Tripathi, B. Chaubey, J. Desire, V. N. Pandey, J.-L. Decout, *J. Med. Chem.* **2004**, *47*, 4806–4809.

[15] a) J. C. Verheijen, B. A. L. M. Deiman, E. Yeheskiely, G. A. van der Marel, J. H. van Boom, *Angew. Chem.* **2000**, *112*, 377–380; *Angew. Chem. Int. Ed.* **2000**, *39*, 369–372; b) L. Petersen, M. C. de Koning, P. van Kuik-Romeijn, J. Weterings, C. J. Pol, G. Platenburg, M. Overhand, G. A. van der Marel, J. H. van Boom, *Bioconjugate Chem.* **2004**, *15*, 576–582.

[16] a) C. Gnaccarini, S. Peter, U. Scheffer, S. Vonhoff, S. Klussmann, M. W. Göbel, *J. Am. Chem. Soc.* **2006**, *128*, 8063–8067; b) U. Scheffer, A. Strick, V. Ludwig, S. Peter, E. Kalden, M. W. Göbel, *J. Am. Chem. Soc.* **2005**, *127*, 2211–2217.

[17] J. Razkin, H. Nilsson, L. Baltzer, *J. Am. Chem. Soc.* **2007**, *129*, 14752–14758.

[18] S. Mikkola, E. Stenman, K. Nurmi, E. Yousefi-Salakdeh, R. Strömberg, H. Lönnberg, *J. Chem. Soc. Perkin Trans. 2* **1999**, 1619–1625.

[19] a) S. Olofsson, G. Johansson, L. Baltzer, *J. Chem. Soc. Perkin Trans. 2* **1995**, 2047–2056; b) S. Olofsson, L. Baltzer, *Folding Design* **1996**, *1*, 347–356.

[20] a) K. S. Broo, L. Brive, P. Ahlberg, L. Baltzer, *J. Am. Chem. Soc.* **1997**, *119*, 11362–11372; b) L. K. Andersson, G. T. Dolphin, J. Kihlberg, L. Baltzer, *J. Chem. Soc. Perkin Trans. 2* **2000**, 459–464; c) L. K. Andersson, M. Caspersson, L. Baltzer, *Chem. Eur. J.* **2002**, *8*, 3687–3697.

[21] a) P. Y. Chou, G. D. Fasman, *Biochemistry* **1974**, *13*, 211–222; b) P. Y. Chou, G. D. Fasman, *Biochemistry* **1974**, *13*, 222–244; c) J. S. Richardson, D. C. Richardson in *Prediction of Protein Structure and the Principles of Protein Conformation* (Ed.: G. D. Fasman), Plenum, New York, **1989**, pp. 1–88.

[22] W. C. Johnson Jr. , *Proteins* **1990**, *7*, 205–214.

[23] P. Ballinger, F. A. Long, *J. Am. Chem. Soc.* **1960**, *82*, 795–800.

[24] An estimate from the method of Takahashi et al. using the p*K*a of the corresponding COOH group of the ribouronic acid (Wu et al.): a) S. Takahashi, L. A. Cohen, H. K. Miller, E. G. Peake, *J. Org. Chem.* **1971**, *36*, 1205–1209; b) J. Wu, A. S. Serianni, *Carbohydr. Res.* **1991**, *211*, 207–217.

[25] a) A. J. Kirby, A. G. Varvoglis, *J. Am. Chem. Soc.* **1967**, *89*, 415–423; b) C. A. Bunton, E. J. Fendler, E. Humeres, K.-U. Yang, *J. Org. Chem.* **1967**, *32*, 2806–2811; c) M. J. Colthurst, M. Nanni, A. Williams, *J. Chem. Soc. Perkin Trans. 2* **1996**, 2285–2291; d) S. A. Ba-Saif, A. M. Davis, A. Williams, *J. Org. Chem.* **1989**, *54*, 5483–5486.

[26] L. K. Andersson, G. T. Dolphin, L. Baltzer, *ChemBioChem* **2002**, *3*, 741–751.

Received: January 28, 2008
Published online on July 4, 2008

